

NATIONAL AERONAUTICS AND SPACE ADMINISTRATION

Technical Memorandum 33-715

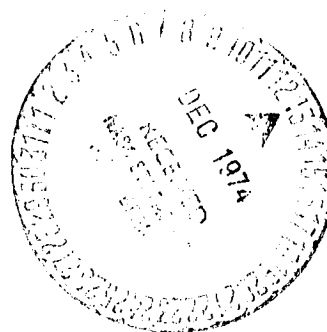
Jupiter Radiation Belt Models (July 1974)

Neil Divine

(NASA-CF-140845) JUPITER RADIATION BELT
MODELS (JULY 1974) (Jet Propulsion Lab.)
15 p HC 43.25 CSCL 03a

N75-12869

UNCLAS
63/90 03564



JET PROPULSION LABORATORY
CALIFORNIA INSTITUTE OF TECHNOLOGY
PASADENA, CALIFORNIA

November 15, 1974

NATIONAL AERONAUTICS AND SPACE ADMINISTRATION

Technical Memorandum 33-715

Jupiter Radiation Belt Models (July 1974)

Neil Divine

JET PROPULSION LABORATORY
CALIFORNIA INSTITUTE OF TECHNOLOGY
PASADENA, CALIFORNIA

November 15, 1974

PREFACE

The work described in this report was performed by the Project Engineering Division of the Jet Propulsion Laboratory under the cognizance of the Mariner Jupiter/Saturn 1977 Project.

CONTENTS

Introduction 1
Electron Models 2
Proton Models 9
References 13

TABLE

1. Parameters for July 1974 Radiation Models 8

FIGURES

1. Radial dependence of electron omnidirectional flux 4
2. Radial dependence of electron omnidirectional flux, with data from San Diego and Chicago experiment packages 5
3. Integral energy spectra representing the electron omnidirectional flux, for four inner values of L 6
4. Integral energy spectra representing the electron omnidirectional flux, for four outer values of L 7
5. Radial dependence of proton omnidirectional flux 10
6. Integral energy spectra representing the proton omnidirectional flux, for four inner values of L 11
7. Integral energy spectra representing the proton omnidirectional flux, for four outer values of L 12

PRECEDING PAGE BLANK NOT FILMED

ABSTRACT

Flux profiles derived from data returned by Pioneer 10 during Jupiter encounter form the basis for a new set of numerical models for the energy spectra of electrons and protons in Jupiter's inner magnetosphere.

INTRODUCTION

Fluxes of energetic electrons and protons in Jupiter's radiation belts, as measured by instruments aboard Pioneer 10 in December 1973, are specified in several articles prepared in May 1974 and published in *Journal of Geophysical Research* (1 September 1974, refs. 1-4). These fluxes represent more thorough and complete reductions of the data than the preliminary fluxes previously available. They include nine electron energy intervals and four proton energy intervals, and confirm important discrepancies in the former below about 10 MeV. Based on the figures in these articles (and on new magnetic dipole parameters for Jupiter, ref. 5), it has been appropriate to generate a new set of numerical flux models for the spacecraft and mission design purposes of the Mariner Jupiter/Saturn 1977 project.

ELECTRON MODELS

Profiles of electron omnidirectional flux J (in $\text{cm}^{-2}\text{s}^{-1}$) are specified in figure 2 of ref. 1 (UC) for energy $E_e > 3$ MeV, in figure 14 of ref. 2 (UCSD) for $E_e > 0.16, 9$ and 35 MeV, and in figure 13 of ref. 3 (UI) for $E_e \geq 0.06, 0.55, 5, 21,$ and 31 MeV as functions of time during the Pioneer 10 fly-by for Jupiter. Using the magnetic dipole specification (D_2) from ref. 5, the Pioneer 10 trajectory has been computed in magnetic coordinates (shell parameter L and latitude λ), and a set of times has been chosen which includes maxima and minima in the flux profiles and equal values of L inbound and outbound. Flux values at these times, read from the profiles, have been tabulated and analysed for dependences on L, λ and E_e ; they are consistent with independence of time and longitude in this coordinate system.

A form for the latitude dependence was chosen which is consistent with a pitch-angle distribution (in the magnetic equator) proportional to $(\sin \lambda)^m$, and values for m were determined by comparing the inbound and outbound flux points at equal values of L . Using $m=4$ for $L < 6.5$ and $m=2$ for $L > 6.5$, the flux data were adjusted to equatorial ($\lambda=0$) values. These adjusted data are plotted as the points figures* 1 through 4, as functions of L and E_e .

Figures 3 and 4, in which integral flux spectra are shown, indicate that some of the data are inconsistent; for example, at $L=3.1$ the points which represent the flux J for $E_e > 0.16$ MeV are below those which represent J for $E_e > 3$ MeV. These discrepancies were the motivation for the creation of two numerical models for the electron fluxes. The high flux model is intended to fit the UI and UC data for the four thresholds $E_e > 0.06, 3, 21,$ and 31 MeV (among which there are no discrepancies), as shown by the corresponding upper lines in figure 1. The low flux model is intended to fit the UCSD data for

* To facilitate comparisons among the figures, common scales are used throughout, such that 2 cm represents one decade in flux J and energy E , and 1 cm represents 1 Jupiter radius in L (except electron flux plots, where 1 cm represents $2 R_J$ in L).

the three thresholds $E_e > 0.16, 9$ and 35 MeV, as shown by the corresponding lower lines in figure 2. The high flux model specifies flux values very similar to those of the Pioneer 10 Workshop model developed in February 1974.

The form used to represent J , the integral, omnidirectional flux (in $\text{cm}^{-2}\text{s}^{-1}$) of particles with energy exceeding E , is

$$\log J = C - Bx + (B-Dx) \frac{E^2}{A^2 + E^2} + \frac{m}{2} \log \left[\frac{(\cos \lambda)^6}{\sqrt{4-3(\cos \lambda)^2}} \right]. \quad (1)$$

Here $x = \log E$ for electron energy $E = E_e$ in MeV and $\log J$ is linear in the parameters B, C, D, β , and m , but not in A . Values for these parameters (all constant or linear in L) are specified for both models in table 1, yielding values for $\log J$ which are also linear in L , within two segments broken at $L = 6.5$. For $E \ll A$, eq. (1) resembles a power law spectrum ($J = 10^C/E^\beta$), and for $E \gg A$, it resembles a different power law spectrum ($J = 10^{B+C}/E^{\beta+D}$). The corresponding differential flux $j = -(dJ/dE)$ in $\text{cm}^{-2}\text{s}^{-1}\text{MeV}^{-1}$ is

$$j = \frac{J}{E} \left[\beta + D \frac{E^2}{A^2 + E^2} - (B-Dx) \frac{2A^2(\ln 10)E^2}{(A^2 + E^2)^2} \right]. \quad (2)$$

The parameter values in table 1 lead to values for J and j which are both positive and continuous in energy for all $E > 0$, within the region $2.85 < L < 15$. For the low flux model, in which data at only 3 energies were fitted, parameter values were selected which minimize j in the energy range $1 < E < 5$ MeV. In those few regions where the low flux model flux exceeds the high one, the smaller of the two fluxes should be taken as the low flux model (the high one stands).

These electron models are plotted as functions of L and E_e in figures 1 through 4, for comparison with the data and with one another. Among the 128 data points fitted for the high flux model, only 6 (corresponding numbers for the low flux model are 79 and 5) differ from the model by more than a factor two (0.3 in $\log J$).

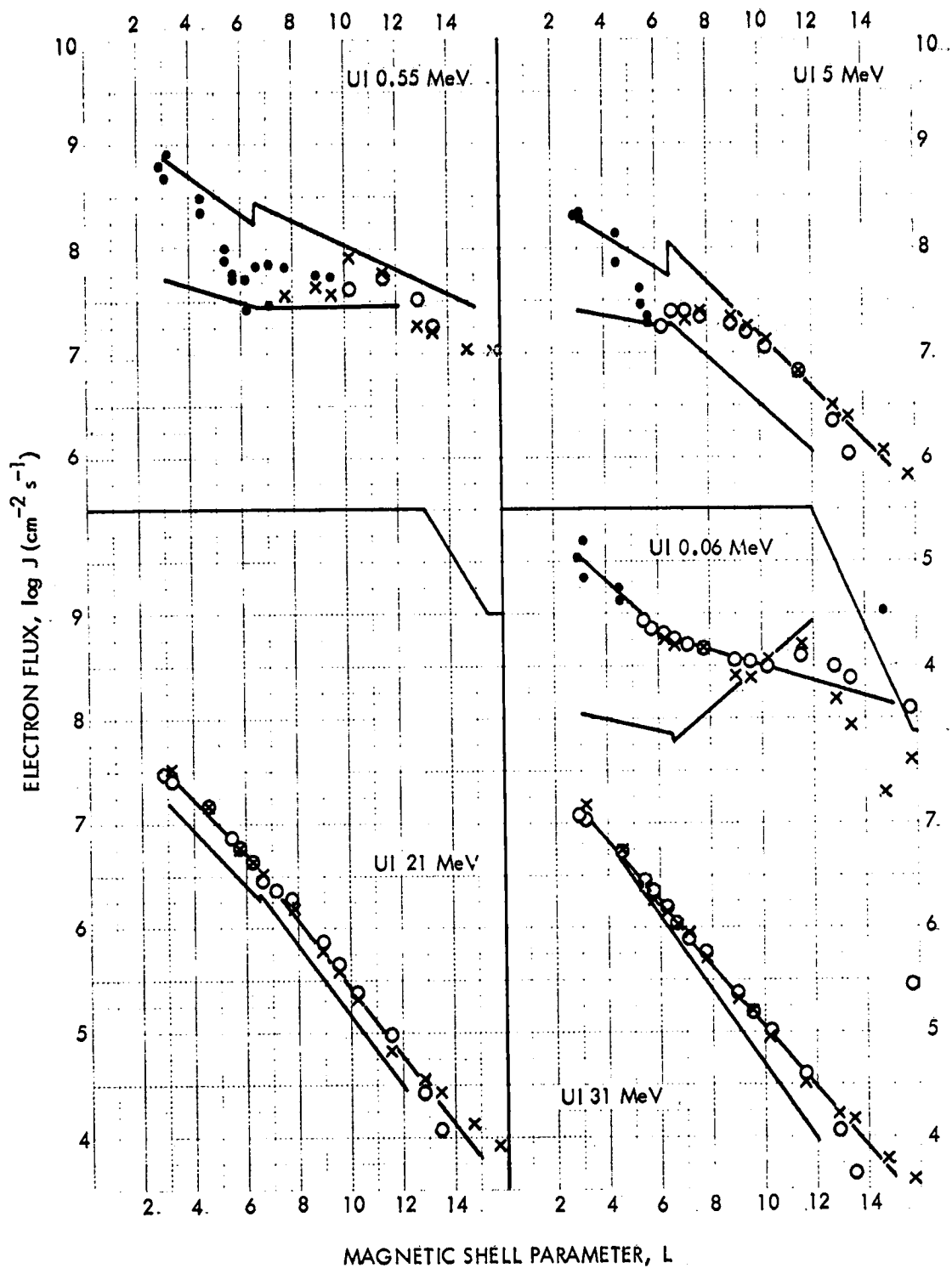


Figure 1. Radial dependence of electron omnidirectional flux. The points represent data for five energy thresholds measured by the Iowa experiment package on Pioneer 10 (\times inbound, \circ outbound, and \bullet less reliable data), adjusted to latitude $\lambda = 0$. The lines represent new high and low flux models.

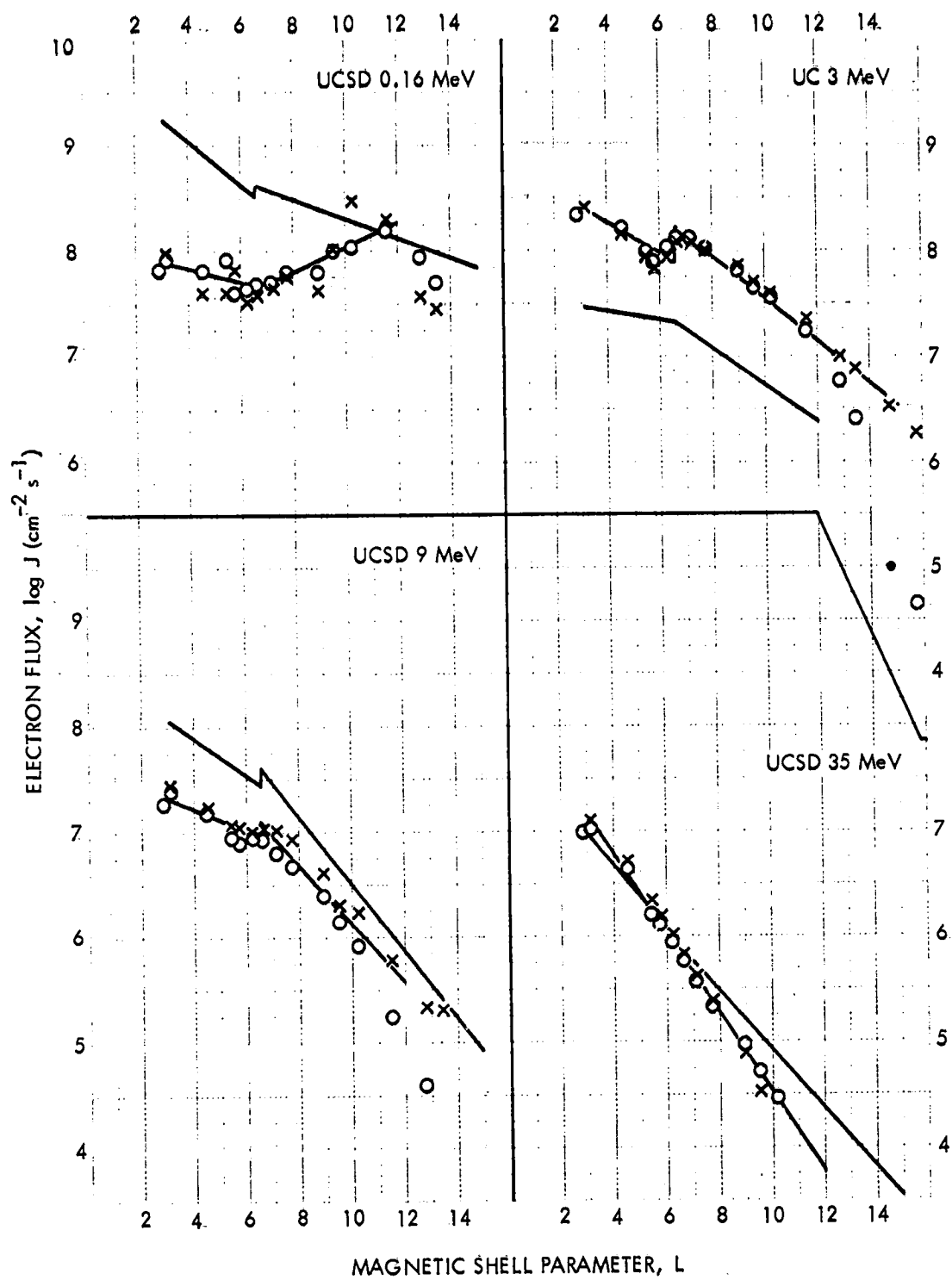


Figure 2. Same as figure 1, with data from San Diego and Chicago experiment packages

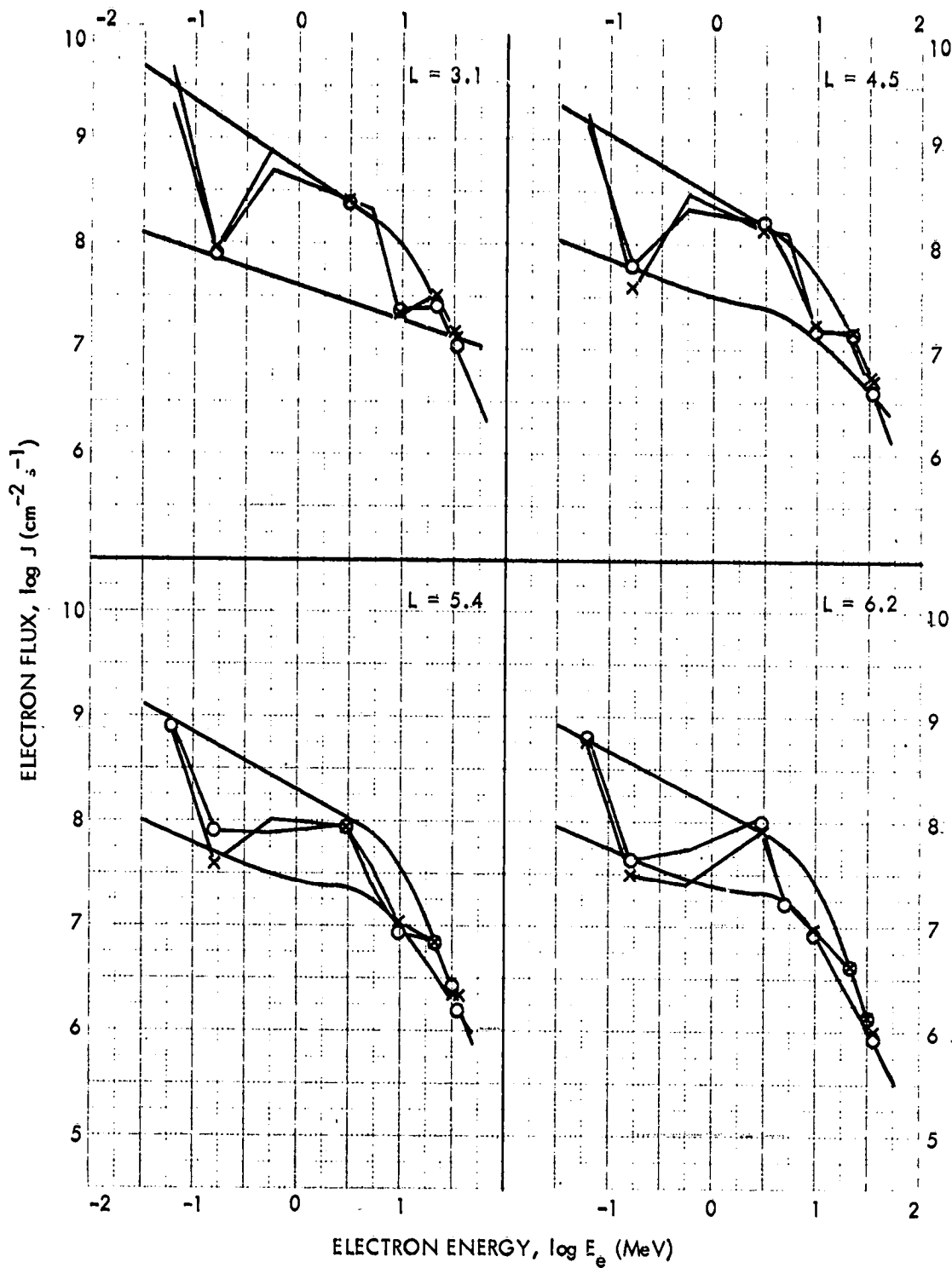


Figure 3. Integral energy spectra representing the electron omnidirectional flux, for four inner values of L , adjusted to $\lambda = 0$. Points and lines as in figure 1.

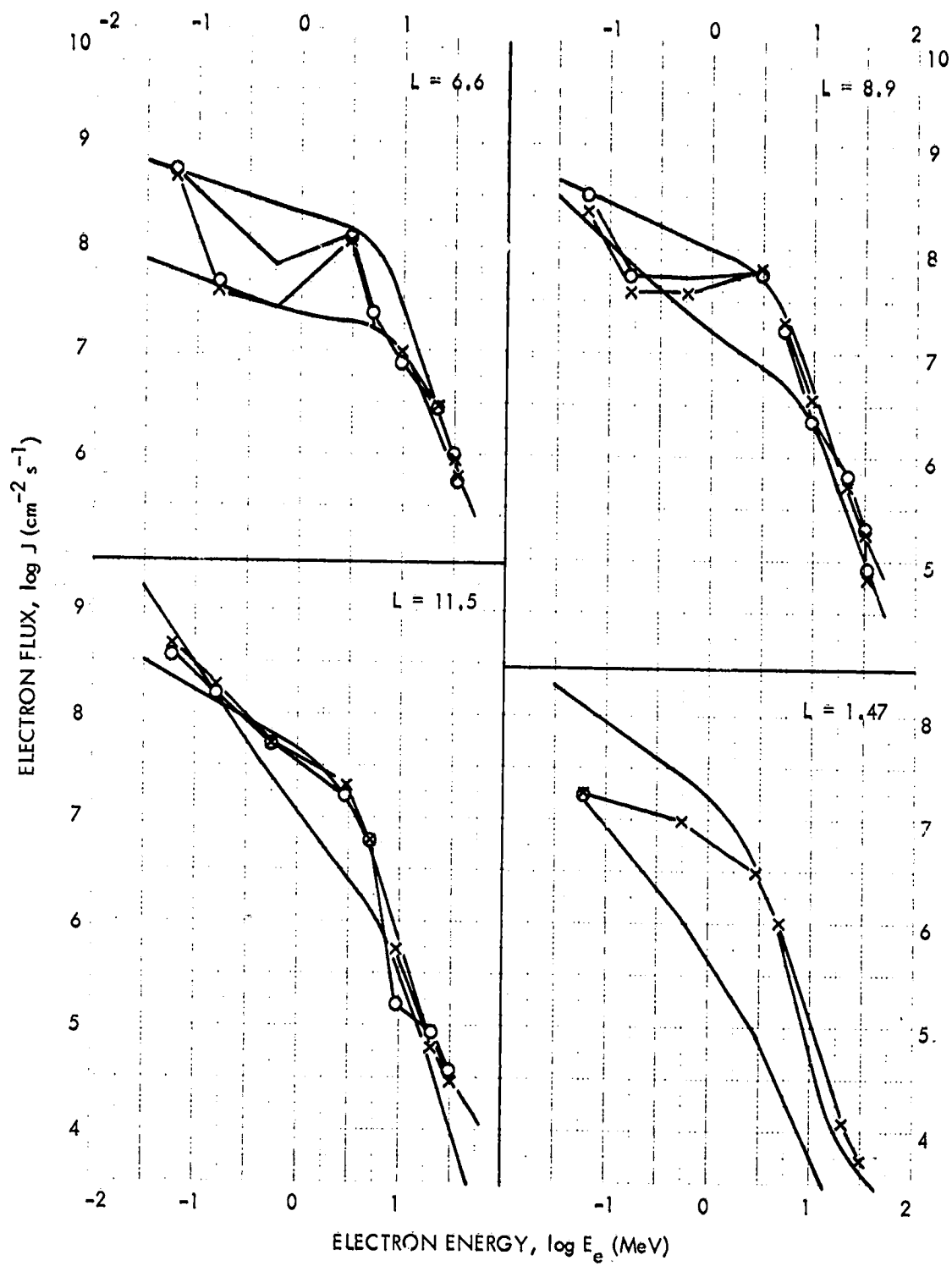


Figure 4. Same as figure 3, for four outer values of L.

Table 1. Parameters for July 1974 Jupiter Radiation Models, to be used with equations (1) and (2); if low flux electron fluxes exceed the high flux ones, substitute the latter.

MODEL	L RANGE	A	B	C	D	β	m
HIGH FLUX ELECTRONS	2.85<L<6.5	15	1.7-(0.15)L	9.21-(0.17)L	1.21+(0.05)L	0.811-(0.048)L	4
	6.5<L<15.0	8	4.99-(0.57)L	9.15-(0.125)L	4.18-(0.31)L	0.047+(0.043)L	2
LOW FLUX ELECTRONS	2.85<L<6.5	5	B=D	7.89-(0.09)L	-1.37+(0.45)L	0.233+(0.031)L	4
	6.5<L<12.0	3	B=D	7.74-(0.06)L	2.44-(0.07)L	-1.139+(0.226)L	2
PROTONS	2.85<L<3.4	60	-67.02+(21.9)L	6.40+(0.39)L	-30.34+(10.62)L	-0.054+(0.13)L	5
	3.4<L<6.0	60	7.95-(0.15)L	9.494-(0.52)L	6.04-(0.08)L	-0.36+(0.22)L	5
	6.0<L<11.0	60	23.6-(1.62)L	9.16-(0.205)L	11.24-(0.51)L	2.25-(0.025)L	4

PROTON MODELS

Profiles of proton omnidirectional flux J (in $\text{cm}^{-2}\text{s}^{-1}$) are specified in figure 2 of ref. 1 (UC) for energy $E_p > 35$ MeV, in figure 15 of ref. 2 (UCSD) for $E_p > 80$ MeV, and in figure 17 of ref. 4 (GSFC) for $1.1 < E_p < 2.15$ and $14.8 < E_p < 21.2$ MeV as functions of time during the Pioneer 10 fly-by of Jupiter. Data from these profiles, processed and adjusted as for the electrons (but using latitude exponents $m=5$ for $L < 6$ and $m=4$ for $L > 6$), are plotted as the points in figures 5 through 7, as functions of L and E_p . There are no major spectral discrepancies among these data, so that a single model is appropriate.

Forms identical to those used for the electrons (eq. 1 and 2) have been used to describe the proton spectra. The fitting procedure for the protons was more cumbersome than for the electrons because two of the four flux profiles represent interval rather than integral values for J . Values for the parameters A , B , C , D , β , and m are specified in table 1, and the models are plotted as the lines in figures 5 through 7. In figures 6 and 7, the horizontal line segments represent the interval J values predicted by the model, for comparison with the corresponding interval data points. As for the electrons both J and j are positive and continuous in energy for all $E > 0$ (for $L > 2.85$), and $\log J$ is linear in L within three segments ($L < 3.4$, $3.4 < L < 6.0$, and $6.0 < L$). Among the 70 data points fitted, only one (inbound $L=6.5$ for $1.1 < E_p < 2.15$) differs from the model by more than a factor two (0.3 in $\log J$).

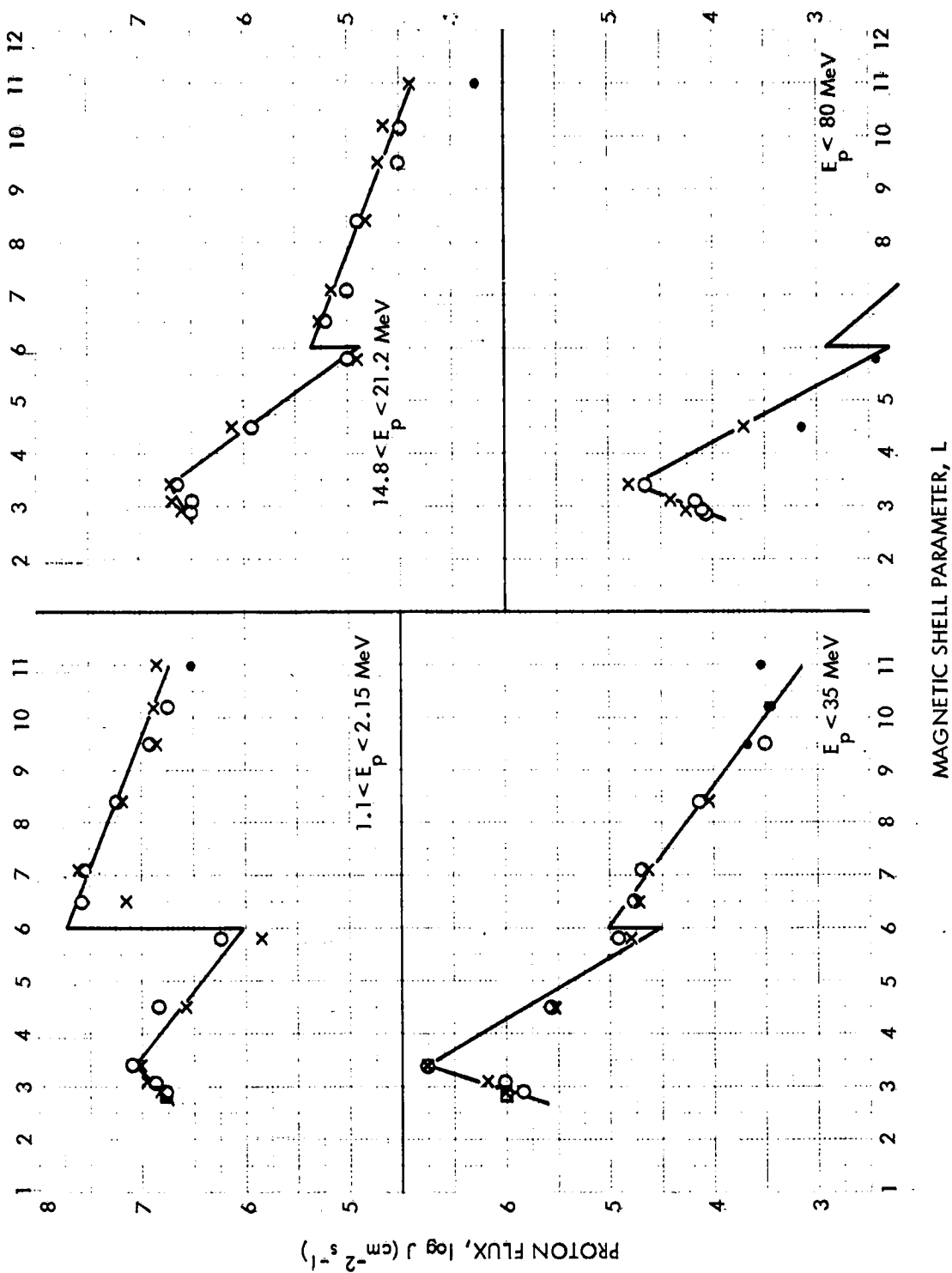


Figure 5. Radial dependence of proton omnidirectional flux. The points represent data in four energy intervals (x inbound, o outbound, • less reliable data), adjusted to latitude $\lambda = 0^\circ$. The lines represent the new proton model.

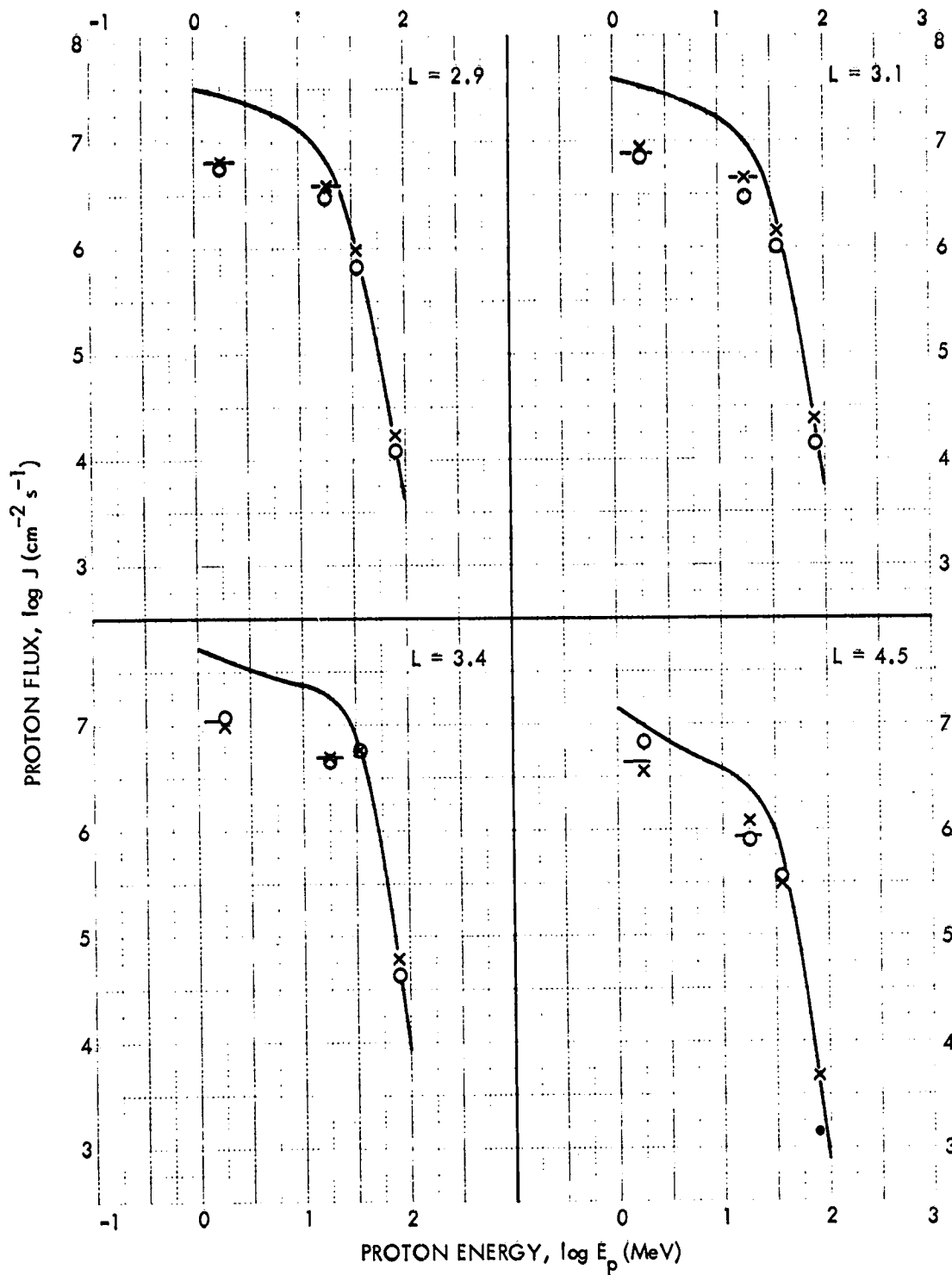


Figure 6. Integral energy spectra representing the proton omnidirectional flux, for four inner values of L . The curves represent the new proton model, as do the horizontal line segments for the two energy intervals $1.1 < E_p < 2.15$ and $14.8 < E_p < 21.2$ MeV. The points represent corresponding data (adjusted to $\lambda = 0$; see fig. 5).

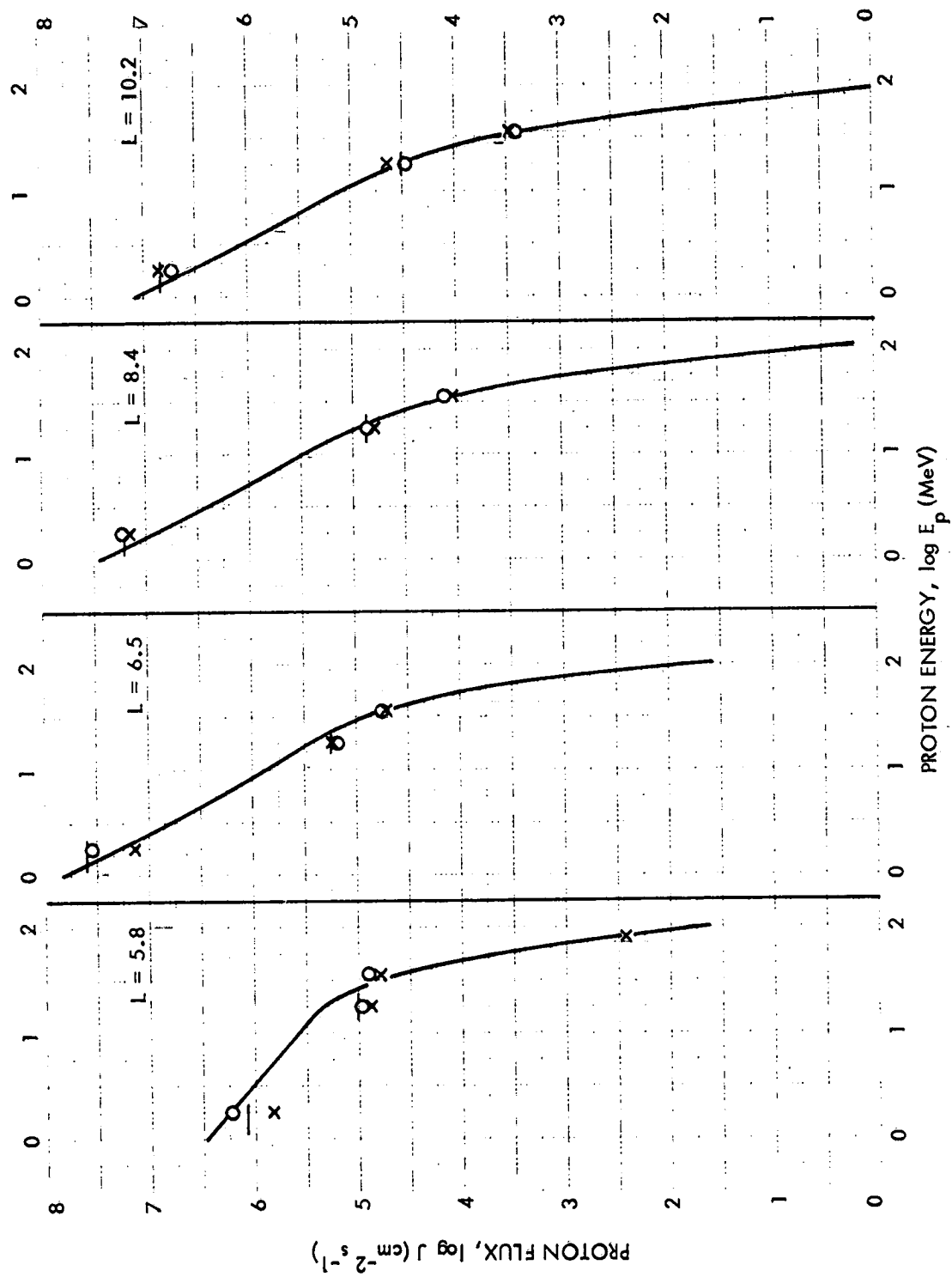


Figure 7. Same as figure 6, for four outer values of L .

REFERENCES

1. Simpson, J. A., *et al.*, 1974: "The Protons and Electrons Trapped in the Jovian Dipole Magnetic Field Region and their Interaction with Io", *J. Geophys. Res.* Vol. 79, No. 25, pp. 3522-3544.
2. Fillius, R. W., and C. E. McIlwain, 1974: "Measurements of the Jovian Radiation Belts", *J. Geophys. Res.* Vol. 79, No. 25, pp. 3589-3599.
3. Van Allen, J. A., *et al.*, 1974: "The Magnetosphere of Jupiter as Observed with Pioneer 10. 1. Instrument and Principal Findings", *J. Geophys. Res.* Vol. 79, No. 25, pp. 3559-3577.
4. Trainor, J. H., *et al.*, 1974: "Energetic Particles in the Jovian Magnetosphere", *J. Geophys. Res.* Vol. 79, No. 25, pp. 3600-3613.
5. Smith, E. J., *et al.*, 1974: "The Planetary Magnetic Field and Magnetosphere of Jupiter: Pioneer 10", *J. Geophys. Res.* Vol. 79, No. 25, pp. 3501-3513.